# MODELING, SIMULATION AND TECHNOLOGY OF MICROBEAM STRUCTURES FOR MICROSENSOR APPLICATIONS

Georgeta IONAŞCU[1], Lucian BOGATU[2], Adriana SANDU[3], Elena MANEA[4], Ileana CERNICA[5]

*Nano/microgrinzile în consolă sunt structuri tot mai des utilizate pentru detecţia de masă în domeniul nano/microsistemelor electromecanice (NEMS/MEMS). Metoda de detecţie rezonantă, tratată în lucrare, se bazează pe modificarea masei sistemului prin adsorbtia substanţelor din mediul înconjurator.*

*In lucrare sunt prezentate aspecte ale modelării, simulării şi fabricării microgrinzilor în consolă, rezonante, cu lăţime constantă/variabilă şi structură multistrat (Si, $SiO_2$, polimer SU-8).*

*Calculul analitic şi simularea numerică, efectuate pentru a determina frecvenţa de rezonanţă a microgrinzilor, oferă o bună concordanţă a rezultatelor obţinute. Sunt prezentate şi rezultatele experimentelor efectuate prin corodarea anizotropă a siliciului utilizând soluţie de KOH de diferite concentraţii.*

*Nano/microcantilevers are structures increasingly utilized for mass detection in nano/microelectromechanical systems (NEMS/MEMS). Resonant detection method, subject of this paper, relies on the change of mass system due to the extraneous substances adsorption.*

*Aspects of modelling, simulation and fabrication of resonant microcantilevers with a constant/variable width and a multi-layered structure (Si, $SiO_2$, polymer SU-8) are presented in this paper.*

*The analytic computation and numerical simulation performed to determine the resonant frequency of the cantilevers offer a good agreement between the results. There are, also, presented the results of the tests performed by silicon anisotropic etching in KOH solution of different concentrations.*

**Keywords:** cantilever beam, mass detection sensor, resonant microstructure

## 1. Introduction

Mass detection can be performed in the nano/micro scale applications by means of some relatively simple devices such as cantilevers, whose experimentally monitored static deflection or resonant frequency variation allows

[1] Prof., Dept. of Precision Engineering, University "Politehnica" of Bucharest, ROMANIA
[2] Assist., Dept. of Precision Engineering, University "Politehnica" of Bucharest, ROMANIA
[3] Prof., Dept. of Strength of Materials, University "Politehnica" of Bucharest, ROMANIA
[4] Dr.Phys., National Institute for R&D in Microtechnology of Bucharest , ROMANIA
[5] Dr.Eng., National Institute for R&D in Microtechnology of Bucharest , ROMANIA

a quantitative assessment of the mass attached to these devices [1]. Static deflection methods are based on the fact that the adsorbed (substance) mass induces a stress gradient into the structure, which causes deformations (deflections) of the beam. The mass being attached, either localized in a point or disposed on a surface in a layer form, can be considered as a gravity force that acts on a beam and generates deflections. Resonant detection methods rely on the change of the sensing system mass (by attachment of extraneous matter) or on the combined modification of mass and rigidity (as the case is of a layer – like deposition), which produces a variation in the fundamental resonant frequency (usually bending or torsion).

Minimal amounts of the deposited mass of femptograms ($10^{-15}$ grams) and even attograms ($10^{-18}$ grams) have already been detected and the promise of downscaling by three orders of magnitude, which is equivalent to molecule-level detection, can only be achieved by very small size devices.

Nano/micro mass detectors are implemented as sensors in a variety of applications such as chemical, biological or clinical analyses, environmental control, monitoring of industrial applications by study of variations in temperature, viscosity, mass, stress or electric/magnetic fields [2]. The initial structure is coated with a (polymer) layer that will retain the substance of interest generally by chemical reactions. This deposition process is followed by mass addition. The difference between the significant variable values (deflection in static methods and frequency change in resonant methods) determined before and after mass retaining constitutes the measure for evaluating the quantity of attached mass.

This paper studies the mass detection by means of the resonant frequency variation method, considering two configurations:

- a microcantilever beam of constant width;
- a microcantilever beam of variable width (paddle cantilever).

The obtaining technology and experimental results for their execution by silicon anisotropic wet etching are presented too.

## 2. Analytic computation

The fundamental frequency for an homogeneous and prismatic cantilever beam of mass $m$, loaded at an end with a concentrated mass $M$ (fig. 1), can be approximately computed by the Rayleigh method [3, 4]:

$$f = \frac{1}{2\pi}\sqrt{\frac{3EI}{l^3(M+0{,}23m)}} = \frac{1}{2\pi}\sqrt{\frac{3EI}{l^3(M+0{,}23\rho Al)}} \tag{1}$$

The following notations were used:

$EI$ – the bending stiffness,

$M$ – the attached mass: $M = M_{polymer} + M_{gas}$ (the polymer is localized in a point and adsorbs selectively a certain gas),

$l$ – the length, $A$ – the cross-sectional area of the beam and $\rho$ – the density of the beam material.

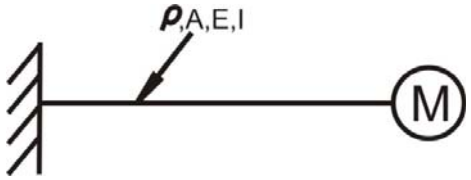


Fig. 1. Model of analytic computation

If the attached mass, $M$, is absent ($M = 0$), the resonant frequency corresponding to the first vibration mode for a cantilever beam results:

$$f_0 = \frac{1}{2\pi}\sqrt{\frac{3EI}{0{,}23\rho A l^4}} \cong \frac{3.61}{2\pi l^2}\sqrt{\frac{EI}{\rho A}} \tag{2}$$

The analysed microcantilever beams are processed by microfabrication technologies specific to the microsensors: the silicon anisotropic wet etching is used to release the microbeam from the silicon substrate (wafer), which acts as a sacrificial material. A boron doped surface layer of silicon works as an etch stop layer. So, the under study microcantilevers, figures 2 and 3, are consequently multilayered structures, with a non-homogeneous (composite) sectional area, the layers succession being given in fig. 4: silicon, silicon dioxide and polymer (SU-8, which is a photoresist layer, too, used in the photolithographic process).

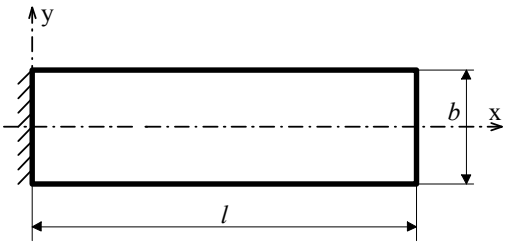


Fig. 2. Microcantilever beam of constant width

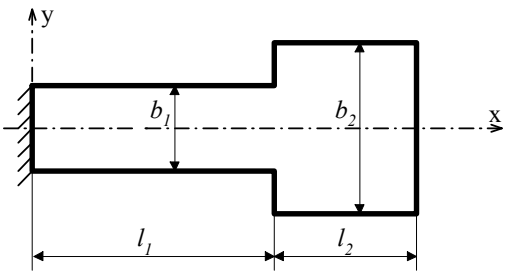


Fig. 3. Microcantilever beam of variable width

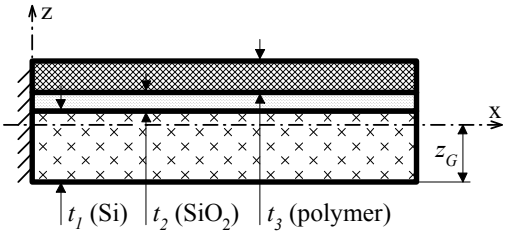


Fig. 4. Succession of layers that compose the microcantilevers; the centroidal axis of the composite beam is marked

In this case, the bending stiffness $EI$ and density ρ are replaced in equations 1 and 2 with the composite bending stiffness $\overline{EI}$ and composite density $\overline{\rho}$:

$$\overline{EI} = \sum_{i=1}^{N} E_i I_i \tag{3}$$

$$\overline{\rho} = \frac{\sum_{i=1}^{N} \rho_i t_i}{\sum_{i=1}^{N} t_i} \tag{4}$$

where: $N$ – the number of layers in the composite cantilever, $E_i$ $I_i$ - the bending stiffness of the individual layers, $\rho_i$ – the density of the individual layers, $t_i$ – the thickness of the individual layers.

The centroid coordinate (the location $z_G$ of the neutral plane) of the composite beam is found by:

$$z_G = \frac{\sum E_i A_i z_i}{\sum E_i A_i} \tag{5}$$

where

$$z_i = \frac{t_i}{2} + \sum_{k=1}^{i-1} t_k \tag{6}$$

$$A_i = b_{ech}\ t_i \tag{7}$$

$$b_{ech} = \frac{b_1 l_1 + b_2 l_2}{l_1 + l_2} \tag{8}$$

$b_{ech}$ – is an equivalent width of a microbeam of constant width and mass equal to that one of the microcantilever of variable width (obviously, $b_{ech} = b$ for the microcantilever of constant width).

$A_i$ – is the cross-sectional area of each individual layer.

The individual moments of inertia $I_i$ of each layer are computed with the following equation:

$$I_i = \frac{b_{ech}\, t_i^3}{12} + b_{ech}\, t_i (z_G - z_i)^2 \tag{9}$$

Replacing $\overline{EI}$ and $\overline{\rho}$ in equations (1) and (2), the fundamental resonant frequency of the composite cantilever beam and its variation after the gas sorption into the polymer layer are obtained:

$$f_1 = f_0 \sqrt{\frac{1}{1 + \frac{M}{0{,}23\overline{\rho} A l}}} \tag{10}$$

$$\Delta f = f_0 - f_1 = f_0 \left( 1 - \frac{1}{\sqrt{1 + K_m}} \right) \tag{11}$$

where $K_m$ is a non-dimensional coefficient (the mass fraction), determined according to the composite cantilever beam mass and the attached mass.

$$K_m = \frac{M}{0{,}23\overline{\rho} A l} \tag{12}$$

The microsensor sensitivity $S$, which represents the frequency variation per unit of added mass by adsorption, can be calculated as:

$$S = \frac{\Delta f}{\Delta M} \tag{13}$$

This equation indicates that in order to obtain a high sensitivity the structure must be sized so that its resonant frequency be high and its equivalent mass ($m_e = \overline{\rho}\ A\ l$) be small. The minimum mass quantity $\Delta M_{min}$, which can experimentally be detected through a minimum resonant frequency variation $\Delta f_{min}$, can be estimated as:

$$(\Delta M)_{\min} = \frac{\Delta f_{\min} (2 f_0 - \Delta f_{\min})}{f_0^2} m_e \tag{14}$$

### 3. Numerical simulation

To optimize the structure geometry in order to obtain a sensitivity as high as possible, parametric models have been performed for both constructive versions presented in figures 2, 3 and 4. Varying one of the parameters and keeping constant the other ones, an analysis of sensitivity can be made. The computations were made considering the following initial data:

- for the microcantilever beam of constant width: $b$ = 80 μm; $l$ = 300 μm;
- for the microcantilever beam of variable width: $b_1$ = 60 μm; $b_2$ = 70 μm; $l_1$ = 150 μm; $l_2$ = 150 μm.

For both of them: $t_1$ (doped Si layer) = 10 μm; $t_2$ ($SiO_2$ layer) = 1.7 μm; $t_3$ (SU-8 layer) = 4 μm. The considered values of elastic and physical constants of the layer materials are given in table 1.

*Table 1*

**Material properties of the layers, which form the composite cantilever beams**

| Material | $E$ [GPa] | $v$ | $\rho$ [kg/m$^3$] |
|---|---|---|---|
| Silicon | 165 | 0.17 | 2330 |
| $SiO_2$ | 70 | 0.17 | 2200 |
| Polymer (SU-8) | 4.4 | 0.22 | 1200 |

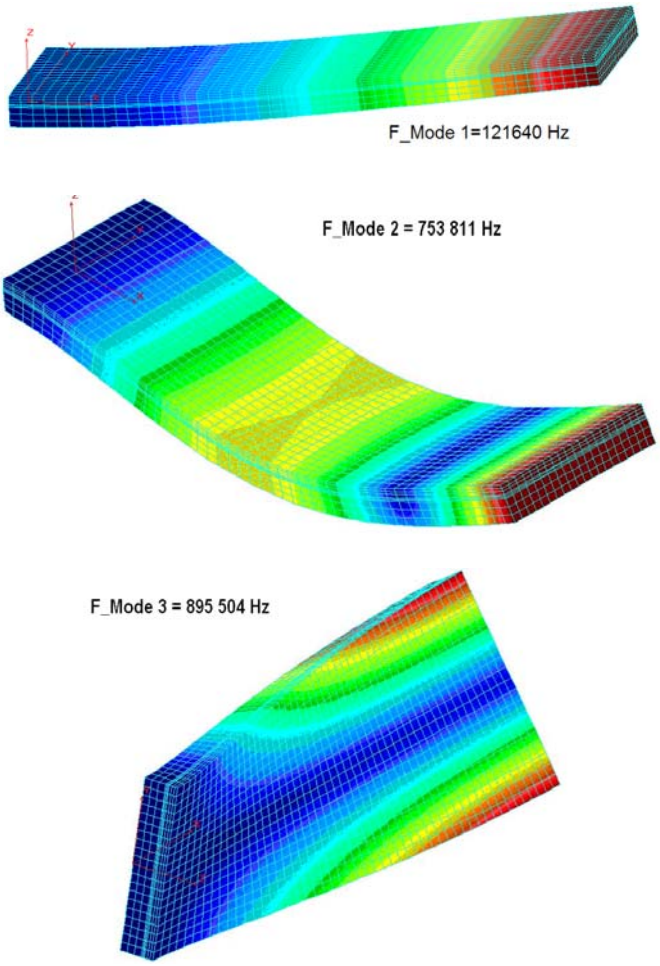


Fig. 5. The first three vibration modes - microcantilever beam of constant width (the first two bending modes and the first torsion mode)

The polymer which adsorbs the gas can be taken in calculation either as a layer deposited on the entire surface of the microbeam (such as we have considered it) or as a mass particle localized in a point-like manner on the

longitudinal direction (symmetrical axis) of the microbeam. The structure meshing was made in elements of three-dimensional solid. Because of the dimensions extremely small of the structures, a convenient choice of the tolerance was made, both for the microstructure geometry description and for its meshing (TOL = $10^{-8} \div 10^{-9}$). The first three vibration modes for both versions of beams are given in figures 5 and 6.

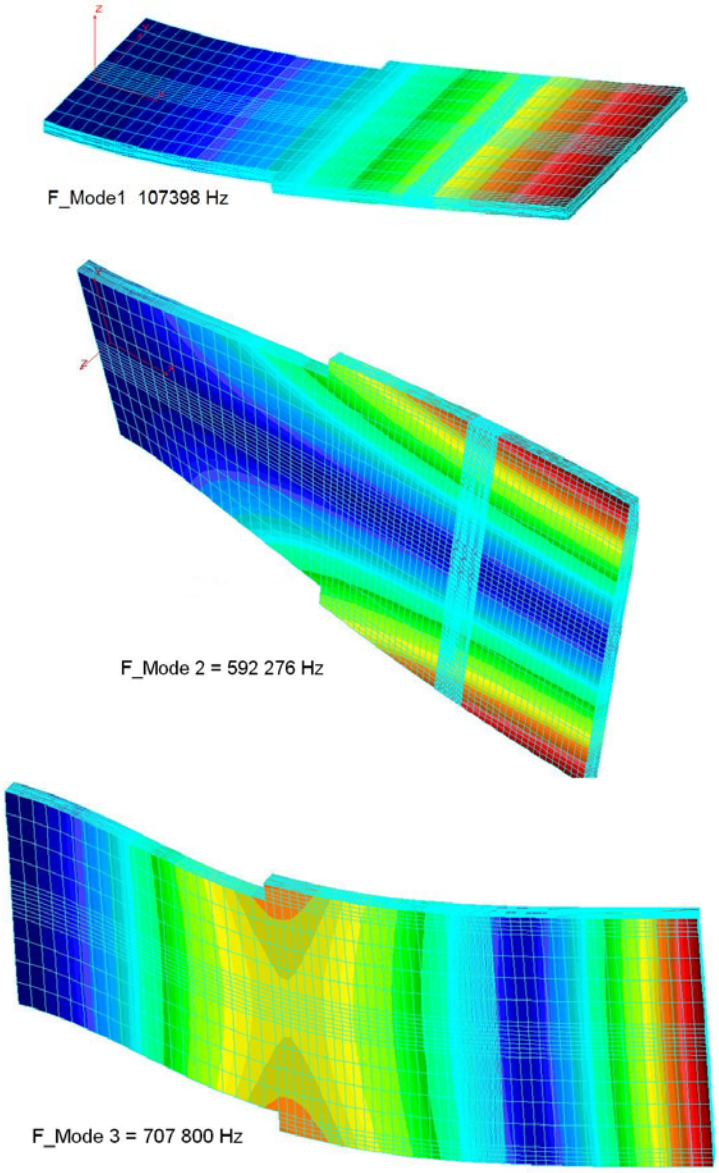


Fig. 6. The first three vibration modes-microcantilever beam of variable width

One can see that the fundamental frequencies are of hundreds of kHz order: 121.6 kHz for the microcantilever beam of constant width and 107.4 kHz for the microcantilever beam of variable width.

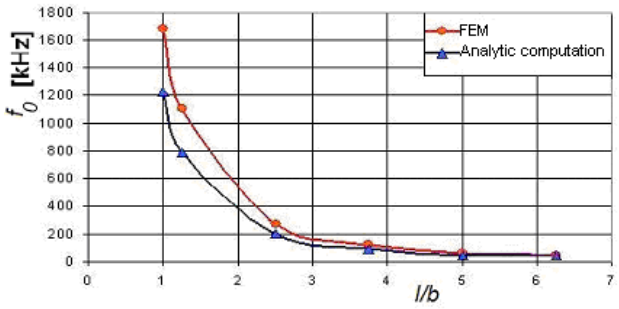


Fig. 7. Comparison between the obtained results analytically and numerically

Fig. 7 presents a comparison between values of the first fundamental resonant frequency for the microcantilever beam of constant width, obtained by using both analytic and numerical computation. As was expected, there is a good agreement between these values for ratios $l/b > 3.5$. For $l/b < 3.5$, the microbeam becomes a "microplate", therefore the bar theory cannot be used.

## 4. Experimental results

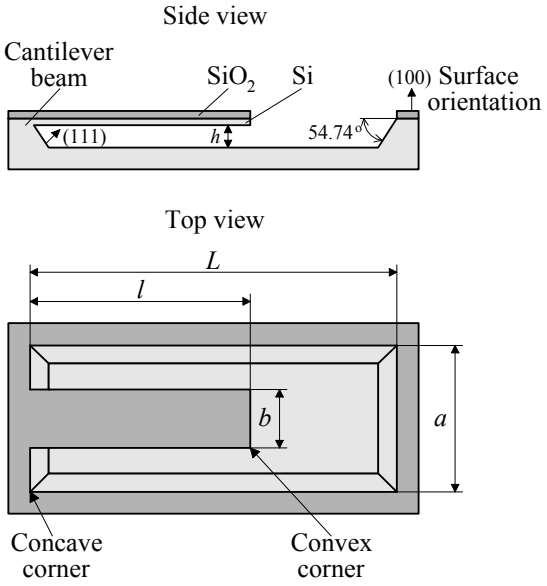


Fig. 8. A pyramidal pit etched in (100) silicon, with an undercut cantilever beam ($a$ = 200 μm, $b$ = 80 μm, $L$ = 500 μm, $l$ = 300 μm, $h$ = 30 μm)

Most liquid-phase etches can be modulated by added dopants in the silicon (boron, in our case), as well as electrochemical biasing, but slow down at the (111) planes regardless of the dopant. It is important to note that from the top view, etching at "concave" corners on (100) silicon stops at (111) intersections, but "convex" corners are undercut, allowing cantilevers rapidly undercut and release. This is illustrated in fig. 8.

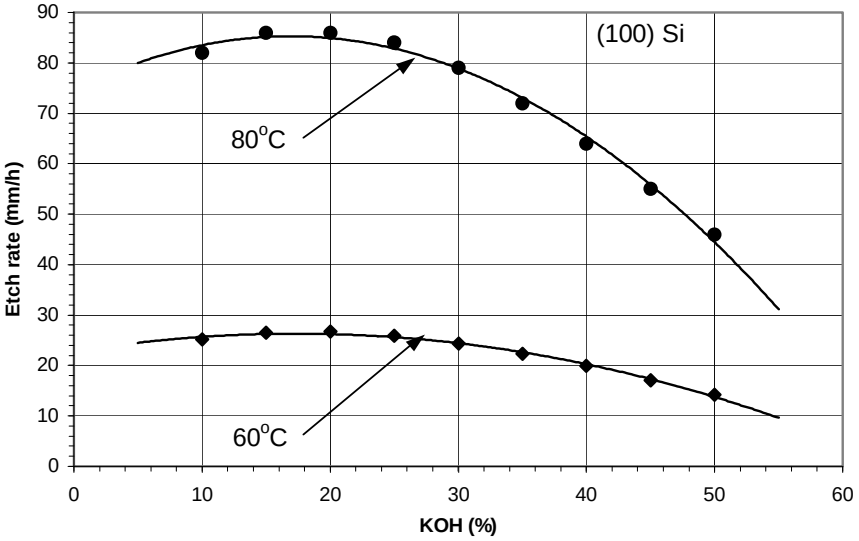


Fig. 9. The etch rate of (100) Si vs. the KOH solution concentration at 60°C and 80°C

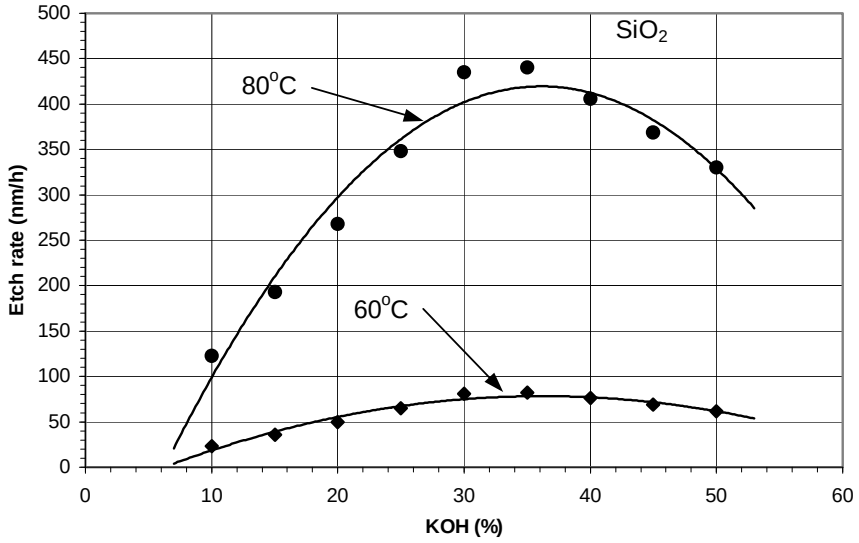


Fig. 10. The etch rate of $SiO_2$ vs. the KOH solution concentration at 60°C and 80°C

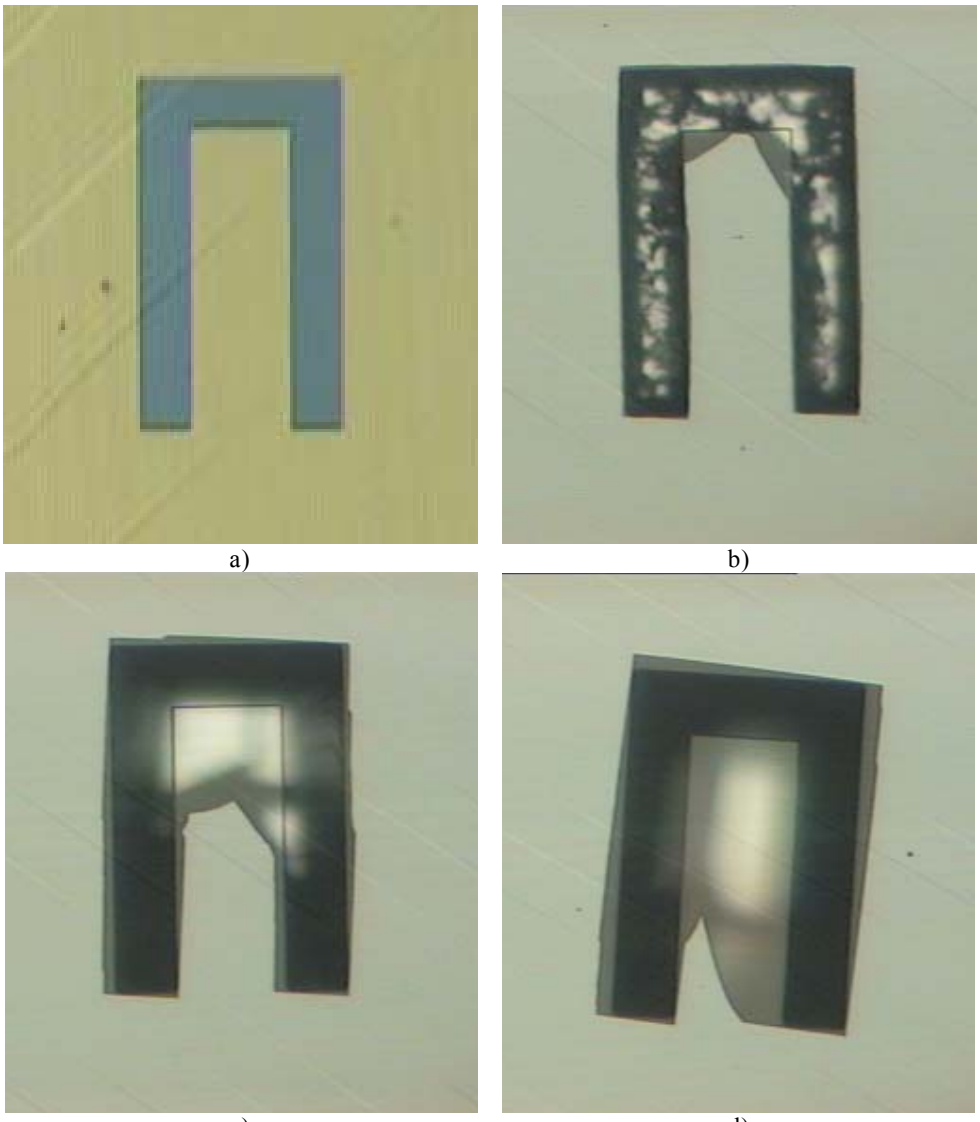

a) b)

c) d)

Fig. 11. Aspects of microbeams executed in (100) Si covered with a protective $SiO_2$ layer before etching (a), and after an anisotropic wet etch (50% KOH, 80°C) in a time of 30 minutes (b), 60 minutes (c) and 90 minutes (d)

More experiments were made in order to determine the etch rates of (100) Si in KOH solution of different concentrations. (100) silicon wafers of p and n-type and (111) silicon wafers were used. They were covered with a $SiO_2$ layer, thermally grown (~1.7÷1.9 μm, oxide thickness) at 1100°C in water vapors (~7 hours). The $SiO_2$ layer is, at the same time, a structural layer and a masking

layer. Its etch was performed in a $NH_4F$:HF solution with a volumetric ratio of 7:1, at 25°C.

We have made dimensional measurements of the depth of the obtained cavities. The measurements were performed comparatively using a microprofilometer ($\alpha$-step) and an optical microscope. The roughness values of the etched surfaces were measured with the Tencor P-1 instrument.

The etch rate and the anisotropy parameters are influenced by the KOH solution concentration, temperature and isopropylic alcohol (IPA) addition. The IPA addition modifies the surface tension of the solution and lightens the release of the hydrogen bubbles from the silicon surface.

The etch rate presents a maximum for a KOH solution concentration between 15÷20% and diminishes continuously at higher concentrations, fig. 9. The KOH solution can be used between the ambient temperature and the boiling point without forming of insoluble reaction products.

It was observed, also, an etch of the $SiO_2$ layer together with the Si substrate in KOH solution, but of a rate much smaller than the Si case is, as results from fig. 10.

Some SEM (Scanning Electron Microscope) photographs, representing microbeams at different etch times, are shown in fig. 11.

## 5. Conclusions

The paper analyses the resonant method of detecting very small quantities of substances that attach to nano/microcantilevers. Two particular configurations have been studied - microcantilever beams with a constant/variable width.

Deposition of extraneous substances on these small-scale structures modifies their resonant frequencies, and direct relationships can be determined between the change in resonant frequency and the mass variation. Several numerical simulations are performed to illustrate various peculiarities of these systems and the resonant frequency shift method.

As regards the experiments performed in order to determine the etch rates of (100) Si in KOH solution of different concentrations, we can infer the following conclusions:

- for KOH solutions, the etch rate of (100) Si does not depend on the substrate doping in the limits of $10^{18}$ $cm^{-3}$ concentration;
- the highest anisotropy ratio is obtained for KOH 25% at 80°C;
- the etch rate in KOH solution significantly raises with temperature and is not influenced by IPA addition;
- the roughness of the etched surfaces reduces by IPA adding.

## REFERENCES

[1]. *N. Lobontiu,* **"**Mass Detection by Nano/Microcantilevers and Bridges", in Acta Technica Napocensis, Series: Applied Mathematics and Mechanics (49), **vol III**, 2006, pp. 509-514.
[2]. *Georgeta Ionascu,* Tehnologii de microtehnica pentru MEMS, Editura Cartea Universitara, Bucuresti, 2004.
[3]. *Gh. Buzdugan (coordonator),* Indrumar de calcul in ingineria mecanica, Editura Tehnica, Bucuresti, 1996.
[4]. *I. Minca, C. Atanasiu, Adriana Sandu, M. Sandu,* Rezistenta materialelor si elemente de teoria elasticitatii, Editura Tehnica, Bucuresti, 1998.